Annales Geophysicae (2004) 22: 1989–2000
SRef-ID: 1432-0576/ag/2004-22-1989

Annales Geophysicae

Dispersive changes in magnetic background noise polarization at 0.1 to 6 Hz during sunset and sunrise at L=1.3

T. Bösinger[1] **and S. L. Shalimov**[2]

[1]Department of Physical Sciences, POB 3000, FIN-90014 University of Oulu, Finland
[2]Institute of Physics of the Earth, 123810, Moscow, B. Gruzinskaya, 10, Russia

Received: 26 September 2002 – Revised: 1 October 2003 – Accepted: 23 January 2004 – Published: 14 June 2004

Abstract. Polarization properties of the magnetic background noise (MBN) and the spectral resonance structure (SRS) of the ionospheric Alfvén resonator (IAR) below the first Schumann resonance but above 0.1 Hz are measured by a sensitive pulsation magnetometer at the island of Crete (L=1.3) and analyzed using the existing SRS theory by Belyaev et al. (1989b). The focus of the paper is on the systematic changes in the MBN and SRS properties associated with the transition from a sunlit to a dark ionosphere (sunset) and vice versa (sunrise). We are able to pinpoint in observations an E-region and F-region terminator effect and to simulate it by means of a simple ionosphere model, implying the formalism given by Belyaev et al. (1989b). The E-region terminator effect is associated with an apparent control for the SRS presence or absence with no clear frequency dispersion in polarization properties, whereas the F-region terminator effect exhibits strong frequency dispersion, especially in the low frequency range. This yields a change in the ellipticity of MBN, starting as early as 2 to 3 h ahead of the "zero-line" of the terminator. In a 24 h presentation of the ellipticity versus frequency and time, the sunrise/sunset effect produces a sharp, dispersive boundary between night and day (day and night). Only inside this boundary, during the night hours, is SRS observed, at times accompanied by a large quasi-periodic long period modulation in the azimuthal angle of the major axis of the polarization ellipse. Attention is also paid to peculiarities in the low frequency range (∼0.1 Hz), where especially large changes in the polarization properties occur in association with the passage of the terminator. The F-region effect is very distinct and well reproduced by our simple model. Changes in the azimuth associated with the E-region terminator effect are of the order of 20°.

Key words. Ionosphere (mid-latitude ionosphere) – Geomagnetism and paleomagnetism (time variations; diurnal) – Space plasma physics (kinetic and MHD theory)

Correspondence to: T. Bösinger
(tilmann.bosinger@oulu.fi)

1 Introduction

It has been established by observations that the main contribution to the horizontal magnetic field of electromagnetic emissions as observed on the ground in the upper ULF and lower ELF frequency range, that is from 1 to approximately 50 Hz, stems from Schumann resonances, Pc 1 magnetic pulsations and a special type of electromagnetic emission that at times reveals the existence of a weak harmonic structure (mostly during nighttime) below and above, but in the vicinity of the first Schumann resonance. This harmonic structure is believed to be a signature of the ionospheric Alfvén resonator (IAR). For a recent collection of IAR related papers, see a special journal issue (J. Atmos. Sol.-Terr. Phys., 62.4., 2000). The properties of this resonator are defined by the local characteristics of the medium along the magnetic field line, primarily in the F-region ionosphere. Conditions for reflection above and below the F-layer maximum can be fulfilled for Alfvén waves in the frequency range between 0.1 and 10 Hz hence, giving rise to standing waves and thereby forming a resonator (Polyakov, 1976; Polyakov and Rapoport, 1981). The lower "wall" of the IAR is at the same time the upper "wall" of the Earth-ionosphere cavity which is responsible for the Schumann resonance. Thus, the frequency characteristics of the impedance of the Earth-ionosphere wave guide upper wall also determines the properties of IAR signatures as, for instance, seen on the ground (Belyaev et al., 1989b).

While the intensity of Schumann resonances is a measure of global thunderstorm activity via electromagnetic emissions from lightning discharges (e.g. Sentman, 1995), the same seems to be true for the harmonic structure of IAR spectra (the so-called spectral resonance structure; SRS) due to their proximity to the first Schumann resonance (Belyaev et al., 1989b), but the SRS is now defined by the IAR's F-region ionospheric properties. In the IAR frequency range a discharge generates an electromagnetic field of TM polarization, for which the ionosphere can be considered as an ideal metallic wall. However, due to a gyrotropic ionospheric sub-layer, a strong local effect takes place which adds to the basic TM mode a TE component. The excitation of IAR takes place by virtue of wave mode conversion from the TM

mode to the Alfvén wave propagating upwards with a subsequent return of an Alfvén wave and energy leakage back to the Earth-ionosphere cavity, due to a wave conversion from the Alfvén wave to the TE mode (Belyaev et al., 1989a, b; Belyaev et al., 1990). It should be mentioned that the IAR theory was independently developed by Lysak (1988, 1999).

The sharp horizontal ionospheric conductance gradient associated with the Earth's terminator and its apparent fast motion overhead of a station anchored at the Earth's surface has made the terminator and the associated effects a popular object of research in various disciplines. In geomagnetic pulsation research (ULF), terminator effects, such as changes in polarization at sunset and sunrise, form a sort of classic research topic (e.g. Saka et al., 1982; Glassmeier, 1984). Also, the ELF community has a great deal of paid attention to a terminator effect ((Barr, 1982), and references therein). Recently, a day-night terminator effect in Schumann resonance properties was discovered (Zieger and Sátori, URSI, 2002).

To our knowledge the first report dedicated to terminator launched gravity wave effects on the spectral resonance structure (SRS) of the ionospheric Alfvén resonator (IAR) is by Ermakova et al. (2000). In this report we step a little bit backward in view of the latter work by addressing only changes in magnetic background polarization properties around the time of the terminator passage over the observation site, leaving gravity wave aspects and other long-term variations in SRS – although well present in our data – out of the scope of the paper. This seems justified, since the primary effect has yet to be explored in more detail before implying larger scenarios. Also, our observations are from a low-latitude station, implying a faster transition between day and night (Bösinger et al., 2002) than in the work by Ermakova et al. (2000). No doubt, the most dramatic changes in ionospheric parameters at mid- and low-latitudes usually take place during the terminator passage. In this report we present and discuss ground-based background magnetic noise measurements in the frequency range from 0.1 to 6 Hz which carry SRS signatures. This is accompanied by corresponding modelling of suspected terminator effects on SRS and magnetic background noise using the basic SRS theory of Belyaev et al. (1989b).

2 Observations

The observations were made with a search coil pulsation magnetometer of the Finnish network (Bösinger and Wedeken, 1987; see http://spaceweb.oulu.fi/projects/pulsations/) that was installed in May 1999 at a remote site in the island of Crete, Greece (35.15° N, 25.20° E, local time LT=UT+1.5 h). The sampling rate is 20 Hz and the Nyquist filter cuts off at about 10 Hz. The three axis instrument is equipped with a GPS clock, providing exact timing of data points close to the nearest second. The system is fully controlled and operated by a PC, with the 12-bit digital data stored on a DAT tape for further processing. Spectral analysis is (if not otherwise mentioned) done with raw data (not corrected for the frequency and phase response of the instrument), since raw data is an advantage in SRS analysis; this is because the increase in sensitivity with frequency counteracts with the decay of background noise amplitude. Quick look, daily dynamic spectra are produced and made available in the web on a routine basis (ftp://spaceweb.oulu.fi/pub/pulsations/Crete/).

By experience the most evident change in ionospheric day- and night-time conditions as they are affecting magnetic background noise between 0.1 and 6 Hz is in the ellipticity ϵ of the horizontal magnetic disturbance vector. This property is shown in Fig. 1 using a color code for one week of data. The ellipticity varies between plus and minus unity, where positive values stand for right-hand and negative values for left-hand polarization. Left and right-hand are here defined according to the gyro-motion of ions (left) and electrons (right) in the Earth's magnetic field. The horizontal axis represents time, with the tick mark indicating the date (day/month) at 02:00 UT (04:00 LT), and the vertical axis represents frequency. Roughly speaking, in terms of colors, daytime is in Fig. 1 characterized by the unstructured, yellow-greenish segments in the figure plane, whereas nighttime is characterized by the highly structured segments with a bluish tone between 0 and 2 Hz and a redish to red one between 2 and 6 Hz. The first Schumann resonance at 8 Hz is artificially depressed. The slightly dispersive, more or less equally spaced, rising structures in the display from early evening to early morning, seen as slanting stripes between 0 and 2 to 3 Hz is what is here (and elsewhere) referred to as SRS. The amplitudes of the resonance enhancements remain usually well below 1 pT but occasionally they can reach 5 pT. One can see that the spacing between adjacent resonance lines is different from night to night and also varies with nighttime. The long period variations of ϵ between 2 and 6 Hz relate with large scale variations in the dark ionosphere, which will be dealt with in a future study.

The sharp transition in Fig. 1 from the daytime unstructured, yellow-greenish segments to the nighttime structured segments with a bluish tone between 0 and 2 Hz and a redish to red one between 2 and 6 Hz defines a demarcation line between day and nighttime which has clearly dispersive characteristics. The transition occurs earlier/later at low frequency from day-to-night/night-to-day and later/earlier at higher frequencies, correspondingly. We called this dispersive demarcation line the "harp-effect" in remembrance of the ancient music instrument and the fact that – to our knowledge – the effect was first observed, at least demonstrated by us, on the basis of data obtained in Crete. The day-night-day demarcation lines represents, so to speak, the body of the harp whereas the IAR resonance lines stand for the strings.

A mere comparison by means of similar plots as the one in Fig. 1, between summer and winter, can tell us that the width of the harp depends on the season: at 1 Hz the width represents in summer about 9 h, whereas in winter it stands for 12 h (cf. Bösinger et al., 2002; their Fig. 2). It would be tempting to identify the harp effect as a terminator effect but this requires further exploration.

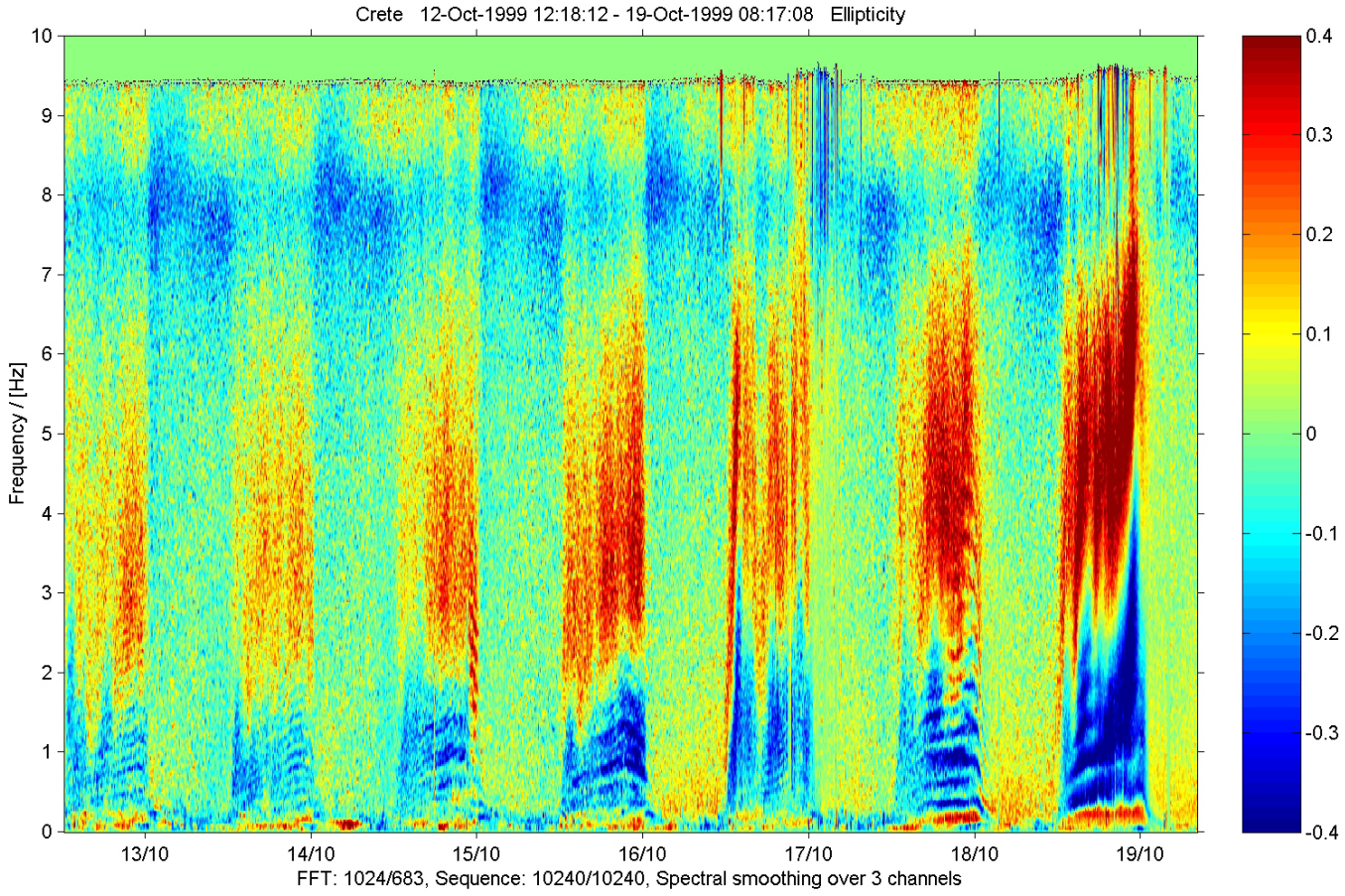

Fig. 1. Dynamic spectra of the ellipticity ϵ of magnetic background noise observed at Crete as a function of time and frequency for a week of data in October 1999. The figure shows the value of ϵ by means of a color code with positive values for right-hand and negative values for left-hand polarized waves. The ϵ parameter is defined between plus and minus unity. Local midnight is UT plus 1.5 h. The tick on the abscissa is at 02:00 UT; the date is of the previous day. For more details see text.

We have in Fig. 2 a closer look at the same type of spectrum as in Fig. 1 but displaying only two successive days, from 17 to 18 October 1999 (which are included in Fig. 1). The color code of Fig. 1 transfers to the grey-scale of Fig. 2 in such a way that totally black refers to plus unity and entirely white to minus unity. In fact, we have at our disposal spectra of the type shown in Fig. 2 for all polarization parameters, such as H (northward), D (eastward), L (left-hand), R (right-hand), ϵ (ellipticity) and ϕ (azimuth of major polarization ellipse) magnetic field components but we show here only the spectrum of ϵ, because it is most sensitive to the type of variation in question (besides ϕ; but this parameter is more difficult to model, see below). What first draws attention are the resonance lines of IAR which are during the night of 17–18 October closer spaced to each other than on the following night (see Fig. 1, cf. also Bösinger et al., 2002). Secondly, the harp effect can be recognized. What follows is a more detailed description of Fig. 2.

A rapid buildup of the F-region layer can be witnessed by a sudden decrease in the resonance frequencies in the early morning of 18 October, at around 04:00 to 05:00 UT. The corresponding solar zenith angles at the station are 97° and 85.8°, respectively; surely in this time the F-region was already sunlit. The decrease in resonance frequency is basically due to an increase in F-peak electron density (Belyaev et al., 1990). Careful inspection of Fig. 2 also reveals that the decrease in resonance frequencies occurs earlier and takes place faster at higher than at lower frequencies (dispersion). This can be understood as a kind of skin-depth effect (see below). The upper ionosphere is hit earlier by sunshine and the effective width of the resonance cavity decreases with time, at least during sunrise. At a later phase the increase of F-peak density will overrule the effect of decreasing resonator width and bring the resonance frequencies down. One may notice in Fig. 2 that the resonance frequencies above 1.5 Hz increased first before they decreased, presumably in conjunction with the buildup of the F-layer peak. At this stage it may already become evident that sunrise/sunset effects on the IAR (which is centered in the F-region) are not processes which run entirely symmetrically to each other in forward or reverse order (sunrise/sunset).

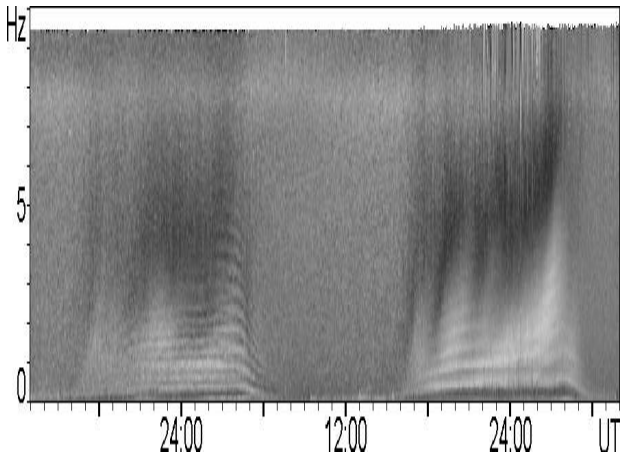

Fig. 2. The same as Fig. 1 but for two successive days (48 h) which are included in the spectrum of Fig. 1. The grey-scale is defined as: totally black stands for plus unity, totally white minus unity. The tick on the abscissa is at 00:00 UT; cf. Fig. 1.

A terminator effect acts differently and at different times on the E- and F-region, respectively. It was shown by Bösinger et al. (2002) that in Crete SRS were observed at every night but never during daytime. This was attributed to the fact that high ionospheric conductance is associated with a low modulation depth in the ionospheric reflection coefficient and consequently, with a low Q-value of the resonator (Trakhtengerts et al., 2000). Thus, strong E-region presence during sunlit hours and its virtual disappearance during dark hours (due to rapid recombination of molecular ions) controls drastically the non-existence of SRS during the day and the existence of SRS during the night. In other words, the E-region conductance operates just like a quench, it suppresses the resonaces during the day and lets it develop during the night. With this background information we look again at Fig. 2.

After sunset the onset of discernable SRS is around 20:00 UT on 17 October, and 3 h earlier, at around 17:00 UT, on 18 October. The solar zenith angle over Crete at these times were 142° and 107°, respectively. Clearly the late appearance of SRS on 17 October must have a different reason than sunset, but on 18 October the appearance of SRS coincides nicely with sunset. The E-region should just about be getting dark when the solar zenith angle is equal or larger than 105°. In other words, an E-region terminator effect should become visible around 17:00 UT. Later, looking further down in time, we can realize an increase in resonance frequencies between 18:00 and 20:00 UT which tells us that during this time the F-region photoionization is greatly diminishing, that means sunset in F-region heights. At this point it is highly suggestive that we identify the demarcation lines forming the harp as a terminator effect. Note that the harp effect is also seen on the previous day at exactly the same time, although an appearance of SRS at sunset and thereafter is blurred by some other reasons (see Discussion).

Inspection of Fig. 2 around the harp effect defining the demarcation lines reveals that the change in ϵ with time is different for the day-night and night-day transition and ϵ behaves differently in different frequencies bands. Keeping in mind the apparent speed of the terminator above the station (1000 km/h), we look at changes in polarization properties on the time scale of typically one hour. Clearly, the temporal extent of the demarcation lines and their dispersive behavior– according to Fig. 2–make these lines an object with considerably, longer duration, something of the order of 2 to 3 h. In the following we look with greater time resolution to the harp effect.

In Fig. 3, from the top to bottom, the panels display in color-coded form (a) total power, (b) the degree of polarization, (c) the ellipticity ϵ, and (d) the azimuth ϕ of the major axis of the polarization ellipse. For more details, see the figure caption. First, we concentrate on the bottom panel. The figure shows data from 18 October alone. In the evening to night sector we can easily distinguish between three different types of phenomena: there are the harmonic SRS structures in brown color, starting around 18:00 UT, and with a slight increase of frequency as time proceeds; there are the quasi-periodic long period variations of ϕ in blue color, starting around 17:00 UT, and there is an only slightly inclined (dispersive), almost vertical slab in intensive brown color. It is tempting to associate this slab with the terminator. Its duration of $\sim$1 h is just about right. Also, it occurs close to sunset. Moreover, thereafter, the SRS comes into appearance. The slap, however, is repeated, although not as intense at around 21:00 UT. In addition, the brownish color started in the low frequency region already around 15:00 UT. What we could identify as an abrupt terminator effect is– below $\sim$3 Hz – the sudden decrease in ϵ values (from $\sim+2$ to ~-2) and a sudden change in azimuth at around 17:00 UT. It interrupts the brownish color development for about one hour, it exhibits dispersion, it occurs at sunset, and SRS starts to develop thereafter (the "quench" is taken off). As will be shown below, we have to distinguish between an E-region and an F-region terminator effect. In summary, what Fig. 3 between is showing us 15:00 and 19:00 UT is the fine structure of the evening demarcation line of Fig. 2. Thus, the demarcation line incorporates the E-region terminator effect but it is a much broader object which includes several phenomena (most likely associated with a F-region terminator effect, see below).

For a test we look in Fig. 4 at a similar spectrum as in Fig. 3 but for the previous day, 17 October (cf. also Fig. 2), the two lowest panels. Signatures of the harp effect can be clearly seen, with the demarcation line starting at the low frequency end already at 16:00 UT! Recall that in Fig. 3 (bottom panel) at the lowest frequency, the brownish region started already at 15:00 UT. This early onset cannot be associated with the E-region terminator effect of Fig. 3. However, later, at $\sim$17:00 UT, we see in Fig. 4 dispersive, abrupt changes in the ellipticity and azimuth angle which we identified in Fig. 3 as the F-region terminator effect.

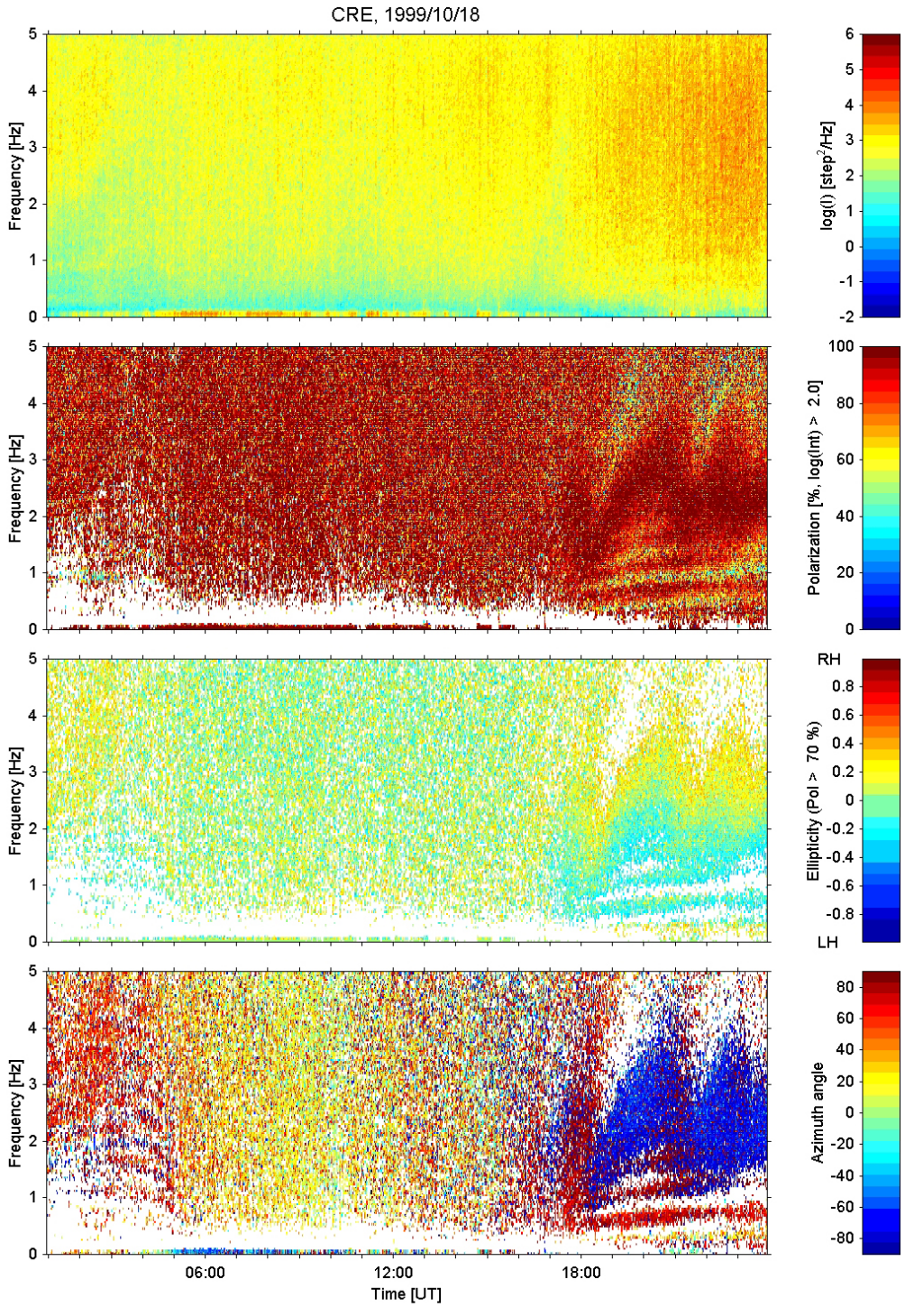

Fig. 3. Upper panel: the power spectral density (PSD) of the magnitude of the horizontal magnetic disturbance (noise) vector in a color-coded form, of arbitrary scale (step or byte to the power of two per Hz). Second panel from above: the degree of polarization in % for all PSD levels above 10^2 in the upper panel. Second panel from below: the ellipticity $\epsilon=(L-R)/(L+R)$, where R and L represent the right- and left-hand circularly polarized components, in color-coded form with "red" for right-hand ($\epsilon=+1$) and "blue" for left-hand ($\epsilon=-1$) circular polarization for all PSD levels with a degree of polarization greater than 70% (see adjacent upper panel). Bottom panel: the angle of the major axis of the horizontal polarization ellipse with the direction of magnetic east in degrees; the angle is counted positively in the counterclockwise direction. for three selected UT sectors (LT=UT+1.5 h). Copyright by AGU.

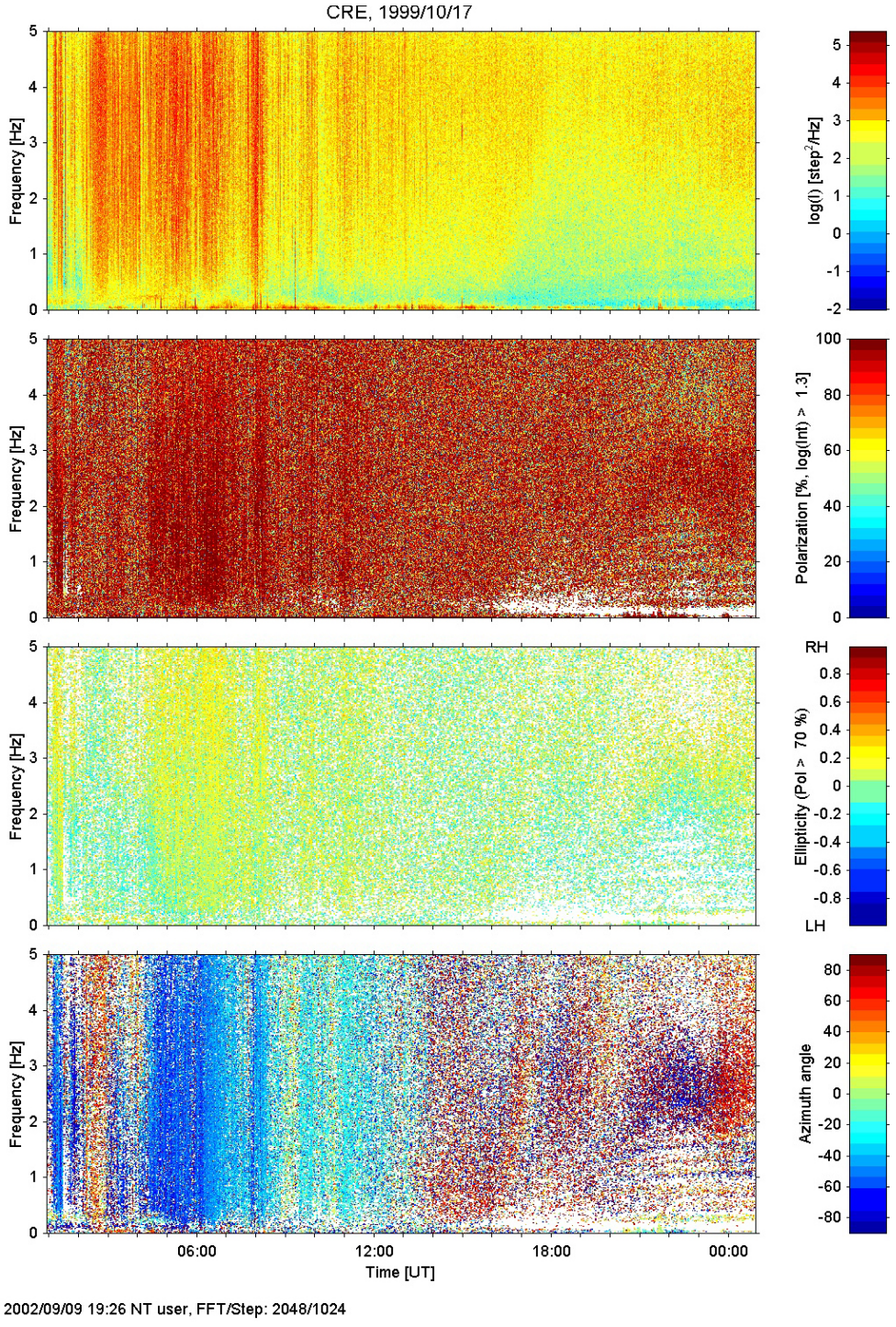

Fig. 4. The same as Fig. 3 but for the previous day; cf. also Fig. 2.

3 A first approach towards a theoretical clarification

In the previous section some experimental evidence was presented for noticeable changes in polarization properties of magnetic background noise around times of sunset and sunrise. Since it is known that in the analyzed frequency range a considerable contribution to the horizontal magnetic field components observed on the ground comes from electromagnetic emissions which are modulated by IAR, we investigate below to what extent the existing theory of IAR can help us to sort out our observations. For this purpose we will first recall in detail the theory developed by Belyaev et al. (1989b). The horizontal components of the magnetic field created in the Earth-ionosphere cavity by electromagnetic waves from distant thunderstorm activity, taking into account mode transformation at the upper "wall" of the cavity, can

be expressed in the quasi-static limit ($k_0 a \ll 1$, $k_0 = 2\pi f/c$, where a is the Earth's radius) by the following approximate formulae (Polyakov and Rapoport, 1981):

$$\frac{H_\theta}{H_\phi} = \frac{\Sigma_H/\Sigma_w}{(\Sigma_P/\Sigma_w + Y) - ik_A h_0\left[(\Sigma_P/\Sigma_w + Y)^2 + (\Sigma_P/\Sigma_w)^2\right]},$$
$$H_\phi = \frac{Il}{2\pi a h_0}, \quad (1)$$

where (θ, ϕ) are spherical angle coordinates, with the polar axis directed towards the lightning discharge, which is located at the point $\theta = 0$, $r = a$ with a current moment Il. Σ_H, Σ_P are the height-integrated Hall and Pedersen conductivities of the E-layer, respectively, $\Sigma_w = cn_A/4\pi$ is the wave impedance, n_A is the Alfvén refractive index in the F-layer, h_0 is the thickness of the insulating gap between the Earth and the ionosphere, $k_A = k_0 n_A$, $Y = (1-R)/(1+R)$ is the admittance of the upper ionosphere, R is the reflection coefficient of Alfvén waves incident on the upper ionosphere from below (Polyakov and Rapoport, 1981). The last term in the denominator of Eq. (1) is a correction term of a more recent formula given by Polyakov et al. (2003). Moreover, the following approximations are made:

$$|R| \approx \exp(-\pi n_e k_A l_H), \qquad arg(R) \approx 2k_A(l_h + l_H) - \pi/2. \quad (2)$$

Here, $n_e = \sqrt{N_{\min}/N_{\max}}$, $N_{\max}$, $N_{\min}$ are the electron densities at the F-layer maximum and in the magnetosphere, l_h, l_H are the characteristic scales of the electron density profile at and above the F-layer maximum, respectively. Notice that the expression for the reflection coefficient R was obtained from the well-known model of the ionospheric wave guide (Greifinger and Greifinger, 1973) which can mimic the actual conditions and represents a flat profile of the F-layer maximum with the thickness l_h and an exponential decrease of n_A^2 with the spatial scale l_H above the flat profile.

Two groups of assumptions were made in order to obtain Eq. (1) (Belyaev et al., 1989b). The first group is concerned with the physical mechanism of TM-mode transformation at the upper wall of the Earth-ionosphere cavity: 1) the ionospheric impedance for the TM-mode field is assumed to be much less than the impedance of the half-space $z < h_0$; thus, the magnetic field component, which is perpendicular to the line of sight source-receiver has no resonant structure, 2) in addition, transformation of the TE-mode into the TM-mode has to be weak, while the backward transformation can be significant, 3) in order for the impedance boundary conditions to be valid locally, the horizontal scale of the ionospheric inhomogeneity L must exceed the Alfvén wavelength in the ionosphere ($k_A L \gg 1$).

The second group of assumptions concerns the derivation of the reflection coefficient R of Alfvén waves (see, Eq. (2): 1) the inequality $k_A l_H \gg 1$ is needed to obtain the expression from a more general equation; it means that the wavelength of the first few eigenmodes should be of the same order as the entire resonator height (the scale length of the inhomogeneity), 2) for the wave reflection in the upper ionosphere, however, a violation of the geometrical optics is needed in form of gradients of the refractive index that are to be steep relative to the wavelength in the medium; it yields the inequality $n_e k_A l_H \ll 1$, 3) in the relevant frequency range the optical thickness of the lower ionosphere has to be small.

4 Numerical estimates

In order to demonstrate the effect of non-uniform horizontal ionospheric conductivity on SRS and polarization parameters of magnetic background noise, a model ionosphere is considered.

To start with a quantitative approach we will use data on the diurnal phase shifts for north-south VLF paths (Chilton et al., 1964), which show that the Earth-ionosphere waveguide makes the transition from day to nighttime propagation conditions in about 60–90 min, during which time the Earth's surface rotates some 1600–2400 km. We use this experimental result in order to 1) conclude that the thickness of the day-night terminator region is greater than the Alfvén wavelength in the ionosphere, and to 2) estimate approximately the characteristic scale of the terminator region as $L \sim 2 \cdot 10^3$ km. Notice, that this spatial scale can also be associated with a time scale for the given terminator velocity.

Although the east-west variation of the ionospheric conductivity is unknown, we assume that in the vicinity of the terminator the distribution of the height-integrated Pedersen and Hall conductivities experience a step-like decrease which is proportional to plasma density. Besides, both the Alfvén refractive index $n_A = c/v_A \sim \sqrt{N_e}$, and the parameter $n_e = \sqrt{N_{\min}/N_{\max}}$ are defined through the electron density at the height of the F-region maximum.

Another parameter that we take into consideration is the scale height l_H characterizing the ionospheric thickness. This parameter demonstrates a rather complex diurnal and seasonal behavior and dependence on the solar cycle (e.g. Titheridge, 1973). For our simplified consideration we use the experimental evidence of the ionospheric thickness increase/decrease at sunset/sunrise (see above).

For the sake of comparison with experimental data, we consider the ellipticity parameter defined as

$$\epsilon(f) = \frac{|H_R| - |H_L|}{|H_R| + |H_L|}, \quad (3)$$

where $H_{R,L}$ are the right- and left-hand circularly polarized magnetic field components which are defined through H_θ and H_ϕ components as $H_{R,L} = \frac{H_\theta \mp i H_\phi}{\sqrt{2}}$.

Next, in order to produce representative numbers, we assume that the plasma density changes as $N_e = N_0(\alpha_N + \beta_N \cdot \tanh(x/L + \gamma_N))$, while the ionospheric thickness as $l_H = l_{H0}(\alpha_l + \beta_l \cdot \tanh(x/L + \gamma_l))$, where N_0, l_{H0} are the plasma density and scale height just before the terminator passage, α, β, γ are model constants, x is the coordinate in the east-west direction normalized by the

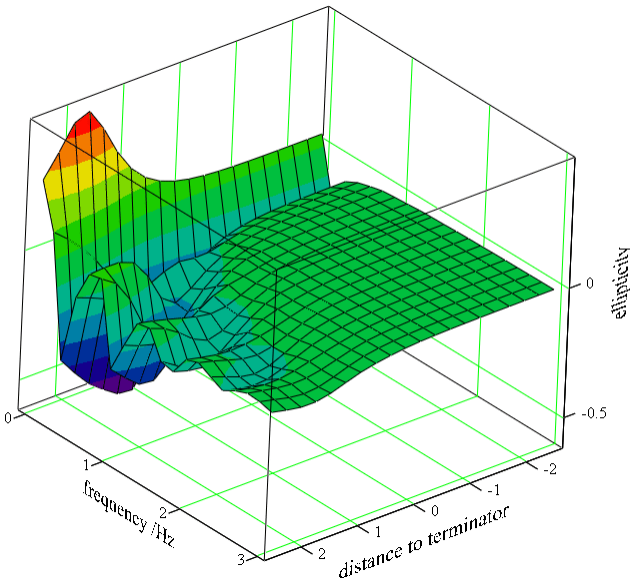

Fig. 5. The ellipticity ϵ as a function of distance (normalized by the terminator characteristic scale L) relative to the terminator's zero-line, as well as a function of frequency for a plasma density proportional to $N_e{=}N_0 \cdot (2/3) - (1/3)\tanh(x/L)$ and an effective ionospheric thickness that changes as $l_H{=}l_{H_0} \cdot \sqrt{3{+}2\tanh(+x/L{-}0.4)}$. Time runs from left to right ($L{=}-2, -1, 0, 1, 2$). For details see text.

characteristic terminator scale. The shift γ is equivalent to a time delay that relates to the non-simultaneous response of the high altitude plasma on the terminator passage.

The formulas for N_e and l_H involve 9 parameters but we are using only one parameter set for which the only variable is x/L, all other parameters are kept constant. In order to be realistic with our parameter choice, we used International Reference Ionosphere (IRI) values of 18 October 1999 (see Figs. 1 and 3; cf. also Fig. 5 in Bösinger et al., 2002) to make a proper tuning. With $N_0{=}10^{11}\mathrm{m}^{-3}$ (IRI at 17:00 UT), $\alpha_N{=}2/3$, $\beta_N{=}1/3$, $L{=}2000$ km, $\gamma_N{=}0$, and $l_{H0}{=}400$ km, $\alpha_l{=}1.2$, $\beta_l{=}0.2$, $\gamma_l{=}0.4$ we obtain across the terminator ($\Delta x{=}4L$) a relative change of N_e by 65% and of l_H by 15%. The corresponding values according IRI (17:00 UT versus 20:00 UT) are 49% and 14%, respectively. As a proxy for l_H we took the exponential decay length obtained from an exponential fit to two values of the IRI electron density height profile, the one of N_0 and of N (1500 km) (cf. Yahnin et al., 2003). Instead of using the ion content as provided by IRI we used a mass loading factor η according to $\eta N_e m_p$ with m_p the proton mass. The factor η was chosen such as to yield approximately the observed resonance frequencies f_A by using the simple formula given below (Belyaev et al., 1989b). Certainly a fit to a specific situation does not yet guarantee the general validity of our parameter set but our model implies only relative changes (across the terminator) which are all very reasonable and where absolute values are used (such as l_h, H_0, Σ_{H0}, Σ_{P0}) they were all checked with IRI to represent typical values. We are heading towards typical features, not towards an event analysis.

$$f_A = \frac{c(k+\frac{1}{4})}{2n_A(l_h+l_H)}, k = 0, 1, 2, ... \quad (4)$$

With the above given parameters (with one exception; see below), using the expressions for N_e and l_H and Eq. (1), (2), (3), $\epsilon(f, x/L)$ was calculated with the result shown in Fig. 5. It displays $\epsilon(f, x/L)$ as function of frequency and time, where time is given in terms of the relative distance to the terminator's zero-line; (see figure caption for more details). Times run from right to left. As can be seen $\epsilon(f)$ exhibits little oscillatory behavior before the zero-line; thereafter, the oscillatory behavior is growing in amplitude, giving rise to the well-known spectral resonance structure. In one parameter we had to make a compromise: the relative change in the Pedersen and Hall conductance relative to the wave conductance had to be larger than described by the relative change in the electron density (65%; see above). This was achieved by using for the electron density connected to the Pedersen/Hall conductance (and only here) $\beta_N{=}2/3$, instead of $\beta_N{=}1/3$; see above. Keeping in mind that the wave conductance is proportional to the square root of the electron density, the additional adjustment seems to be justified and not artificial. With our parameters the adjustment results in a crossing over of the Pedersen/Hall conductances, over the wave conductance when passing from the sunlit to the dark ionosphere. Again, this seems very reasonable.

It can be seen from Fig. 5 that in the vicinity of the approaching terminator the ellipticity $\epsilon(f, x/L)$ exhibits a sort of dispersion, in agreement with the experiment. The changes in $\epsilon(f, x/L)$ start first at low frequencies and then expand to higher frequencies. The whole process takes approximately one unit of relative distance, corresponding to approximately one hour in time with the characteristic velocity of the terminator but the lowest frequencies "sense" the terminator well ahead of the zero-line. The resonant structure appears close to the terminator with eventually growing amplitudes in $\epsilon(f, x/L)$ towards nighttime hours.

The occurrence of this dispersion in $\epsilon(f, x/L)$ finds its explanation in terms of the inequality $n_e k_A l_H \ll 1$, which is assumed in the derivation of the ionospheric reflection coefficient. It indicates a violation of the validity of geometrical optics. Indeed, the inequality is first valid for low frequencies. In consequence this leads to a suppression of all other than resonant frequencies, due to the Alfvén resonator.

In earlier SRS studies we did not try to identify the IAR's fundamental frequency and concentrated instead on the frequency scale Δf, the difference between adjacent resonance frequencies. This is because Pi 1 magnetic pulsations, well represented in our data, easily mask the fundamental frequency of the SRS spectrum (the red traces in the lowest two frequency bins of, for example, Fig. 1 are mostly Pi 1 pulsations, especially at nighttime). However, the behavior of our model in the vicinity of $\sim$0.1 Hz ("zero-frequency") calls now for some attention. For this end in Fig. 6 the ellipticity is again plotted as a function of frequency but only for

three instances: before, at and after the passage of the terminator (as defined by L=−2, 0, +2). The deep minimum of ϵ around 0.1 Hz seen in Fig. 6 is a characteristic for all daytime spectra, best seen in Fig. 1 for 17 October 1999 but also on 13, 14, 15, 16, 18 October and many others of our spectra, plus the steep increase to positive values at around 0.2 Hz, extending in an asymptotic fashion to high frequencies (note we are looking at the daytime spectra). This is in agreement with the red trace in Fig. 6, with the only exception that the ϵ values do not reach far enough to become positive. The deep minimum in ϵ at the low frequency end can be regarded as reminiscent of IAR during daytime conditions. This minimum preserves at the transition from the day-to nightside but its frequency increases steeply after the passage of the terminator (cf. Fig. 6). This is in full agreement with observations (cf. Fig. 1). When proceeding from day to nighttime ("before" to "after", in Fig. 6) the biggest change in ϵ for all frequencies occurs – according to our model – just at the lowest frequencies: from the minimum value around −0.4 (before the terminator, red trace) ϵ jumps up to a positive value around +0.4 (after the terminator, black trace). It looks like that this is also supported by our observations; best seen again on 17 October in Fig. 1: from the blueish region (−0.4) at the bottom frequency during daytime, we hit at sunset a pronounced ϵ maximum in red (+0.4). A similar feature is also seen on 18 October and less distinct, but qualitatively similar, on the other days/nights of Fig. 1.

We should, however, not stress too much the equivalence between model results and observations. First, our model is still very crude, secondly, at the low frequency end, there is this contamination with Pi 1 pulsations, and finally, we are operating at the limit of the SRS model's applicability ($k_A l_H \leq 1$). Still Eq. (2) gives a correct qualitative behavior of R for a "good" as well "bad" resonator. It should also be noticed that the behavior of ϵ above 2 or 3 Hz is not explained by our model (cf. Figs. 1 and 6). It seems that other than IAR effects are dominating in this frequency range.

Finally, a note on the "Harp-effect": The overall impression in Fig. 1 when (below 2 Hz) comparing night with daytime is that nighttime is primarily "blueish", whereas daytime is primarily "yellow-greenish". It means that the minima (not maxima) of ϵ determine the overall blueish tone of nighttime in Fig. 1. Thus, the sharp transition from day-to nighttime, giving rise to the "Harp-effect", is due to the sudden drop in ϵ (cf. Fig. 1). This can be nicely used in Figs. 3 and 4 to determine in the spectra the time of terminator passage.

For the keen eye we present in Fig. 7 a kind of summary of the many observational facts which were addressed above. The opportunity provides spectra of the same kind and of the same day as in Fig. 3 but with emphasis on the lower frequency part with corresponding higher spectral resolution. The Pi1/2 type of pulsations were weak on 18 October, at least in Crete, and do not interfere (they are visible in the lowest frequency bin in the top panel (total power) of Fig. 7). We recognize the dispersive boundary in ϵ from 0.2 Hz upward around 16:00–17:00 UT, the deep, low frequency daytime

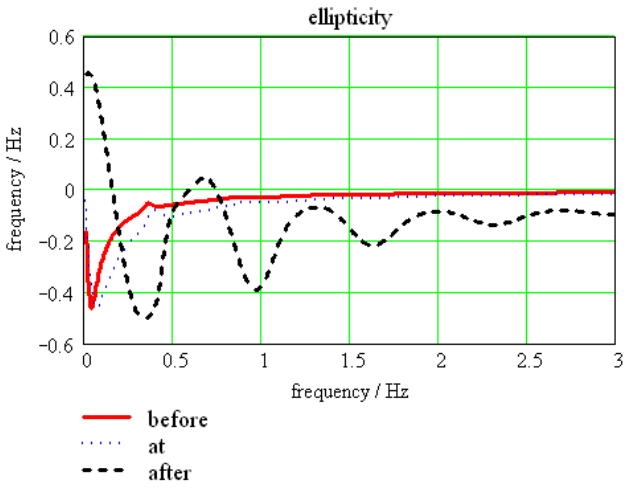

Fig. 6. The ellipticity ϵ as a function of frequency for three instances of time as given by the relative distance of the terminator to the nominal zero-line; before (L=−2), at (L=0), and after (L=+2).

minimum of ϵ migrating rapidly from 0.1 Hz to 0.3 Hz between 15:00 and 18:00 UT, the relatively sudden appearance of a distinct, low frequency maximum of ϵ around 18:00 UT (cf. Fig. 5), the SRS appearing around 18:00 UT), the weak change of ϕ when ϵ becomes "bluish" (it is not the brownish boundary; see above). Finally, a note on the degree of polarization: the average over frequency is practically constant; with the appearance of SRS only a redistribution takes place. The degree is enhanced at the resonance frequencies at the expense of the frequencies apart from the resonances.

5 Discussion

On average, there are at any time about 100 lightning discharges per second worldwide. The basic theory on SRS formation deals with a single discharge. One has in principal to sum-up over any single discharge contribution and integrate over the entire range of viewing angles. If one takes into account the simultaneous action of several source regions from different viewing angles, SRS preserves in the amplitude of the magnetic field (Demekhov et al., 2000) but not in the ellipticity, nor azimuth. Moreover, at low latitudes the polarization can also depend on the angle between the direction to the source and the magnetic meridian plane. Fortunately, when dealing with the time period of sunset at the geographic longitude of the island of Crete, it is safe to say that the main contribution to the magnetic background noise stems from the African sector which is also known to be the strongest thunderstorm activity region worldwide. In this case the H_θ component in Eq. (1) coincides rather nicely with the magnetic noise component towards magnetic north and H_ϕ with the one towards magnetic east. It happens that this is also the orientation of the search coil sensors of our pulsation magnetometer. This makes the interpretation of the orientation of the major axis of the polarization ellipse with respect to the

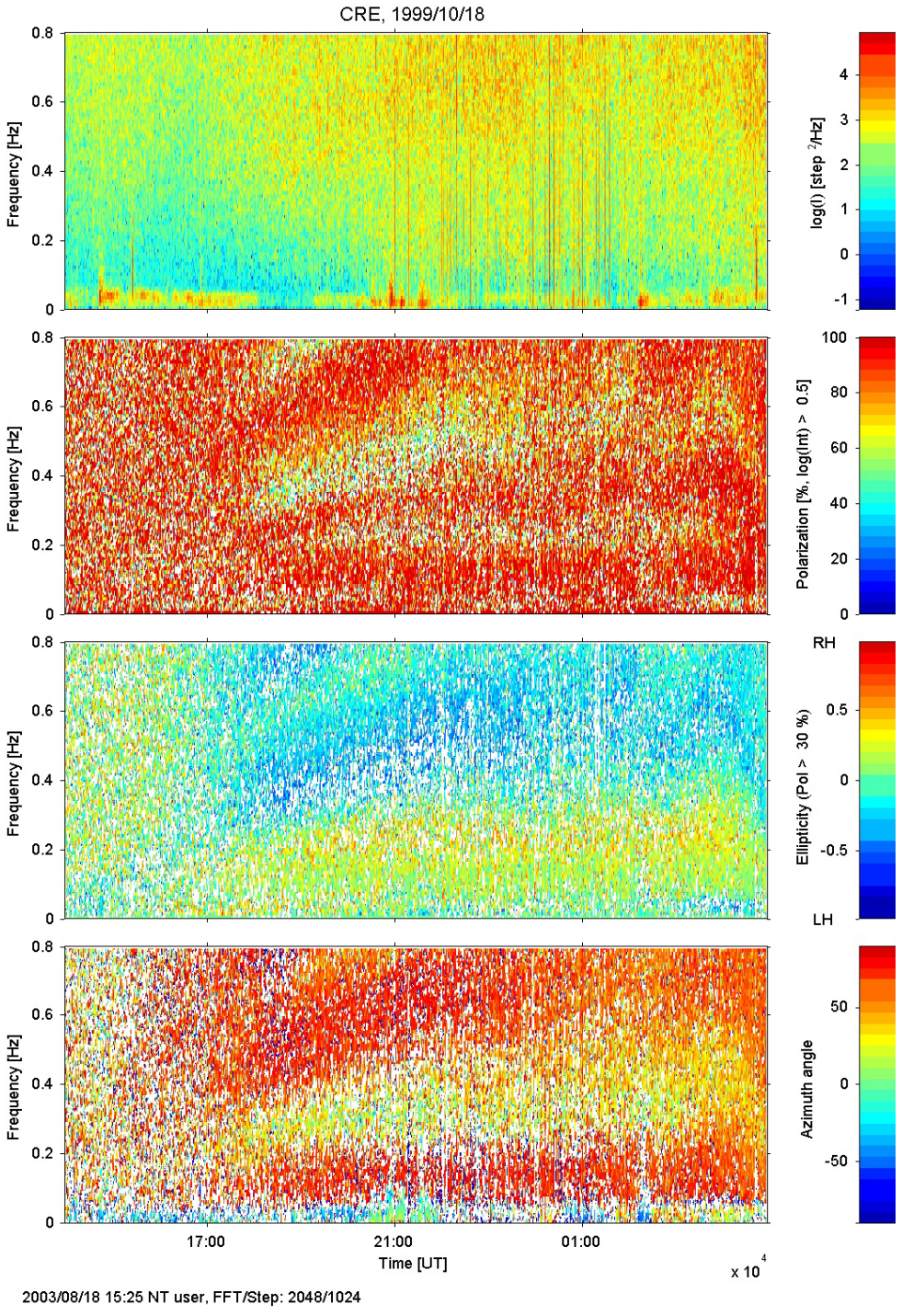

Fig. 7. The same as Fig. 3 but for the low frequency part alone, and with a time axis extending to the morning of the following day; compare also with Fig. 1.

direction of the line of sight to the source region relatively simple. The angle ϕ=90 of the major axis of the polarization ellipse in Figs. 3 and 4 is equivalent to the orientation of the major axis towards magnetic north (parallel to H_θ).

Comparison of the demarcation lines between day and night (night and day) of Fig. 1 (harp effect) with the higher resolution Figs. 2, 3, 4 and 7 revealed that the transition from day to night (night to day) is a manyfold process with a duration of several hours. It includes what we identified as a "terminator effect", but is at times associated with an initiation of a long period modulation of magnetic background noise (probably associated with gravity waves or mesoscale Travelling Ionospheric Disturbances; cf. Fig. 3; see also Ermakova et al., 2000; Garcia et al., 2000). We pinpointed the

terminator effect by two criteria: it should be of a duration of about one hour (comparable with the passage of the terminator above the station) and it should occur around the time when the E-region becomes dark (solar zenith dips below 105°), with corresponding consideration/values for sunrise. Careful inspection of sunset and sunrise in the parameters of ϵ and ϕ in Figs. 3 and 4 and many other similar plots (not shown) taught us that the terminator effect as defined by the criteria mentioned above, is a minor effect best depicted by a change in ϵ (below 2 to 3 Hz to more negative, and above this frequency to more positive values and a change of ϕ of the order of 20° from the pre-existing value (which could be any due to superposition of other effects). We identified these effects as an E-region terminator effect. Our simulation above showed us, however, that the dispersive signatures in ellipticity in the low frequency range, including the "zero-frequency" effect, are long lasting effects with an apparent "sensing" of the terminator already well ahead of the terminator zero line (cf. Fig. 5). We associated this phenomenon with an F-region terminator effect exhibiting a nice correspondence with our observations (harp effect). Its explanation is straightforward and given above. It is associated with a systematic change in the effective width l_H of the resonator at sunset and sunrise, respectively, and the disappearance of the resonator for "zero-frequency", whose value depends on the value of l_H.

6 Summary and Conclusions

The most dramatic effects at sunset are the appearance of SRS and at times, the initiation of long period modulation in ellipticity of magnetic background noise between 1 and 6 Hz. In this paper we do not deal explicitly with these phenomena. The former has already been described and analyzed in literature to a considerable extent. The latter is left for future studies. The motivation to this study arose from presentation of the type shown in Fig. 1 and the discovery of what we called the "harp effect". By means of the existing theory developed first by Belyaev et al. (1989b), we were able to reproduce the main features of this phenomenon. Observations, as well theory, allow us to distinguish between an E-region and F-region terminator effect. In the course of this study it has become apparent that the transition between day and night (night and day) causes a manyfold response in the magnetic background noise polarization properties and in the SRS. The features described and modelled above form only a subset of the many signatures to be addressed in future, in greater detail experimentally, and by more realistic models, theoretically. Our model is very simple and implies only the basic formalism of first order (cf. Pokhotelov et al., 2001). Its success in explaining some basic polarization properties in a quasi-quantitative manner was more a surprise than an expectation. It emphasizes again the power of the pioneer work carried out almost two decades ago by Pavel Belyaev and his co-workers.

Acknowledgements. The author T. Bösinger greatly acknowledge the support by the INTAS99-0335 grant. The author S. L. Shalimov thanks the Academy of Finland for support on the basis of a bilateral exchange programme between Russia and Finland. We are very much obliged to C. Haldoupis for supporting the pulsation magnetometer station in the grounds of the Kallerghi, Hagios Ioannis Monastery. We wish to express our gratitude to the Bishop of Arkaloxwriou-Kastelliou and V. Andreas and the monks of the monastery Father Timotheos and Father Leondios for their enthusiastic support and for allowing the housing of the pulsation magnetometer at the Monastery. Also we are grateful to I. Karavalakis and I. Katzagiannakis, friends and supporters of the Kallerghi Monastery, for their extremely valuable help for the unobstructed operation of our experiment. Support was also provided by M. N. Yakunin and J. P. Valti by spectral analyses and plotting procedures.

Topical Editor M. Lester thanks two referees for their help in evaluating this paper.

References

Barr, R.: The nocturnal D-region as seen by VLF radio waves, J. Atmos. Terr. Phys., 44, 407–413, 1982.

Belyaev, P. P., Polyakov, S. V., Rapoport, V. O., and Trakhtengerts, V. Y.: Experimental study of the resonance spectrum structure of atmospheric electromagnetic background noise in the range of short-period geomagnetic pulsations, Izvetiya vuzov: Radiophysika, 32, 663–672, 1989a.

Belyaev, P. P., Polyakov, S. V., Rapoport, V. O., and Trakhtengerts, V. Y.: Theory of the formation of resonance structure of the atmospheric electromagnetic background noise in the range of short-period geomagnetic pulsations, Radiofizika, 32, 802–810, 1989b.

Belyaev, P. P., Polyakov, S. V., Rapoport, V. O., and Trakhtengerts, V. Y.: The ionospheric Alfvén resonator, J. Atmos. Terr. Phys., 52, 781–787, 1990.

Belyaev, P. P., Bosinger, T., Isaev, S. V., Trakhtengerts, V. Yu., and Kangas, J.: First evidence at high latitudes for the ionospheric Alfven resonator, J. Geophys. Res., 104, 4305–4318, 1999.

Bösinger, T. and Wedeken, U.: Pi1B type magnetic pulsations observed simultaneously at mid and high latitudes, J. Atmos. Terr. Phys., 49, 573–598, 1987.

Bösinger, T., Haldoupis, C., Belyaev, P. P., Yakunin, M. N., Semenova, N. V., Demekhov, A. G., and Angelopoulos, V.: Spectral properties of the ionospheric Alfvén resonator as observed at a low latitude station (L=1.3), J. Geophys. Res., 107, A10, 1281, doi:10.1029/2001JA005076, 2002.

Budden, K.G.: Radio Waves in the Ionosphere, University Press, Cambridge, Mass., 1961.

Chilton, C. J., Crombie, D. D., and Jean, A. G.: Phase variations in VLF propagation, Propagation of Radio Waves at Frequencies Below 300 Kilocycles: Proceedings of the Seventh Meeting of the AGARD Ionospheric Research Commitee, Munich, 1962, edited by Blackband, W. T., 257–290., Pergamon, New York, 1964.

Demekhov, A. G., Belyaev, P. P., Isaev, S. V., Manninen, J., Turunen, T., and Kangas, J.: Modelling the diurnal evolution of the resonance spectral structure of the atmospheric noise background in the Pc 1 frequency range, J. Atmos. Solar-Terr. Phys., 62, 257–265, 2000.

Ermakova, E. N., Belyaev, P. P., Belova, N. I., and Trakhtengerts, S. V.: A sunset effect in variations of the eigenfrequenies of

the ionospheric Alfvn resonator, J. Atmos. Solar-Terr. Phys., 62, 249–252, 2000.

Glassmeier, K.-H.: On the influence of ionospheres with non-uniform conductivity distribution on hydromagnetic waves, J. Geophys., 54, 125–137, 1984.

Garcia, F. J., Kelley, M. C., Makela, J. J., and Huang, C.-S.: Airglow observations of mesoscale low-velocity traveling ionospheric disturbances at mid-latitudes., J. Geophys. Res., 105, 18 407–18 416, 2000.

Greifinger, C. and Greifinger, P.: Waveguide propagation of micropulsations out of the plane of the geomagnetic meridian, J. Geophys. Res., 78, 4611–4618, 1973.

Lysak, R. L.: Theory of auroral zone Pib pulsation spectra, J. Geophys. Res., 93, 5942–5946, 1988.

Lysak, R. L.: Propagation of Alfvén waves through the ionosphere: Dependence on ionospheric parameters, J. Geophys. Res., 104 10 017–10 030, 1999.

Pokhotelov, O. A., Khruschev, V., Parrot, M., Senchenkov, S., and Pavlenko, V. P.: Ionospheric Alfvén resonator revisited: Feedback instability, J. Geophys. Res., 106, 25 813–25 823, 2001.

Polyakov, S. V.: On properties of an ionospheric Alfén resonator, Symposium KAPG on Solar-Terrestrial Physics, Vol. III, Reports, Part 3, 72–73, Nauka, Moscow, 1976.

Polyakov, S. V. and Rapoport, V. O.: Ionospheric Alfvén resonator, Geomagnetism and Aeronomy, 21, 610–614, 1981.

Polyakov, S. V., Ermakova, E. N., and Yakunin, M. N.: The theory of polarization of ultra-low frequency electromagnetic background, Geomagnetizm and Aeronomiya, 42, 240–248, 2003.

Saka, O., Itonaga, M., and Kitamura, T.: Ionospheric control of polarization of low-latitude geomagnetic micropulsations at sunrise, J. Atmos. Terr. Phys., 44, 703–712, 1982.

Sentman, D. D. and Frazer, B. J.: Simultaneous observations of Schumann resonances in California and Australia: evidence for intensity modulation by the local height of the D-region, J. Geophys. Res., 96, 15 973, 1991.

Sentman, D. D.: Schumann resonances, Handbook of Atmospheric Electrodynamics, 1, 267–295, 1995.

Trakhtengerts, V. Y., Demekhov, A. G., Belyaev, P. P., Polyakov, S. V., Ermakova, E. N., and Isaev, S. V.: A mechanism of anticorrelation in the occurrence of ULF electromagnetic noise resonance structure and Pc 1 magnetic pulsations through the solar activity cycle, J. Atmos. Solar-Terr. Phys., 62, 253–256, 2000.

Titheridge, J. E.: The slab thickness of the mid-latitude ionosphere, Planet. Space Sci., 21, 1775–1793, 1973.

Wait, J. R.: Electromagnetic Waves in Stratified Media, 2nd edition, Pergamon Press, Elmsford, N. Y., 1970.

Yahnin, A. G., Semenova, N. V., Ostapenko, A. A., Kangas, J., Manninen, J., and Turunen, T.: Morphology of the spectral resonance structure of the electromagnetic background noise in the range 0.1–4 Hz at L=5.2, Annales Geophysicae 21: 779–786, 2003.

Zieger, B. and Sátori, G.: CXXVIIth General Assembly of the International Union of Radio Science, 17 August–24 August, Maastricht, The Netherlands, 2002.